

Envelope-Flip Dynamics in CpCo(Diene) Complexes: an ab Initio Quantum Mechanical Study

Kim K. Baldrige, Joseph M. O'Connor, Ming-Chou Chen, and Jay S. Siegel*

Department of Chemistry, University of California-San Diego, La Jolla, California 92093-0358

Received: July 12, 1999; In Final Form: October 4, 1999

Ab initio quantum mechanical methods are brought to bear on the problem of syn/anti isomerization of the terminal hydrogens in $(\eta^5\text{-C}_5\text{H}_5)\text{Co}(\eta^4\text{-1,3-cis-butadiene})$ by an envelope-flip process. The first experimentally determined barrier to pairwise syn/anti interconversion in a group VIII highly substituted metal–diene complex is reported. Remarkable agreement between computational and experimental barriers is obtained. A path of stereoisomerization involving two discrete steps, ring flipping and inversion of pyramidality at cobalt, is elucidated in preference to a planar envelope-flip transition state. These results clarify the stereospecific rearrangement observed in two substituted diene derivatives.

Studies on olefin stereoisomerization are as old as the hills,¹ and often serve as the testing ground for new experimental and theoretical methods.² Even investigation of the simple conversion of *cis*- to *trans*-butene caused initial concerns that provoked serious questions in the area of activated transition state theory.^{3,4} The original work using the method of mixed melting points,³ which was later revealed to be indiscriminate between isomerization and decomposition processes, produced erroneous activation parameters that had theorists in a whirl.² The advent of IR spectroscopy and a hard-working team of Harvard undergraduates resolved this problem by focusing specifically on the butene isomerization process.⁴ The work highlighted the need to consider the mechanistic possibilities as well as the nature of intermediates and products when conducting even such simple investigations.

Contemporary problems in olefin stereoisomerization include the influence of metal coordination, a feature that facilitates isomerization and adds mechanistic complexity. In particular, metal–diene complexes have a rich stereochemistry and are of synthetic and industrial importance. Tetrahapto-*cis*-diene complexes may be formally viewed as one of two limiting structures, σ^2, π -form **1** and π, π -form **2**, in which the terminal substituents occupy either syn or anti positions (Figure 1).⁵ Early-metal and actinide complexes have been observed to thermally interconvert syn and anti hydrogens by a process which has been suggested to involve ring inversion via planar metallacyclopentene structure **3** (Figure 2).^{6–8} The free energies of activation for this process in early-metal and actinide complexes fall in the range 6.5–14.3 and 10.5–17 kcal/mol, respectively. For early-metal complexes, which tend to display ground state structures leaning toward form **1**, structure-dynamics correlations have been used to explain the relative rates of interconversion.⁹

In contrast to early-metal and actinide diene complexes, thermal pairwise syn/anti interconversions for the group VIII metals are rare and thus far have been observed only for cyclopentadienyl cobalt complexes at elevated temperatures.^{10–12} The parent complex in this series, $[(\eta^5\text{-C}_5\text{H}_5)\text{Co}(\eta^4\text{-cis,cis-1,4-dideuteriobutadiene})]$ (**4-ZZ**), fails to undergo syn/anti isomerization below 140 °C; and, at higher temperatures stereorandomization occurs.^{12–14} Notably, when **4-ZZ** is irradiated at –96 °C with a krypton ion laser, a rapid, stereospecific equilibration

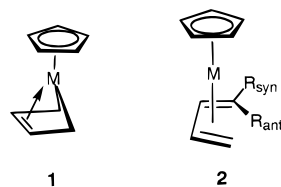


Figure 1. Two limiting forms of a CpM(diene) complex.

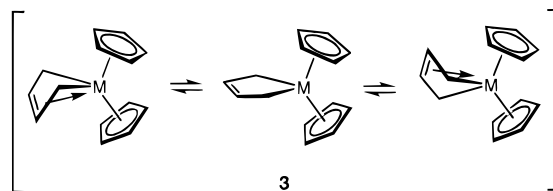
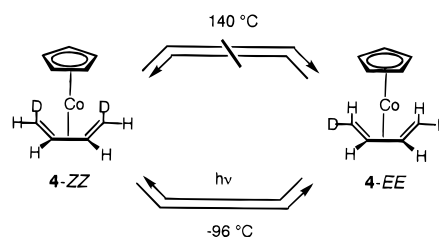


Figure 2. Proposed envelope-flip process for early-metal and actinide diene complexes.

SCHEME 1



with the *trans,trans*-dideuteriobutadiene complex, **4-EE**, is observed; with no formation of the **4-EZ** or **4-ZE** isomer (Scheme 1).¹³

We recently reported the first examples of a pairwise thermal syn/anti isomerization for a group VIII metal (Scheme 2).^{10,11} Thus, in the absence of light, the highly substituted cobalt diene complexes $(\eta^5\text{-C}_5\text{H}_5)\text{Co}[\eta^4\text{-cis,trans-CH(R)=C(SO}_2\text{Ph)C(TMS)=CH(R)}]$ (**5-ZE**, where R = CO₂Et, COMe, CPh, and CO₂C₄H₇) all undergo a slow isomerization in benzene at elevated temperatures (>70 °C) to give the corresponding *EZ*-diene; with no formation of the *ZZ* or *EE* isomers (Scheme 2).^{10,11}

Two 16-electron intermediates, **6**^{13,15} and **7**,^{13,16,17} have been suggested as possibilities for pairwise syn/anti interconversions

SCHEME 2

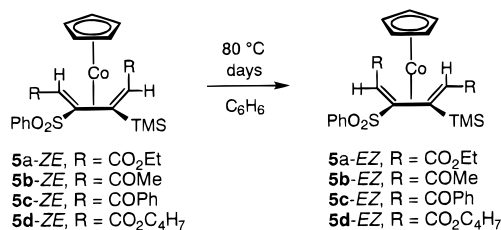


(Figure 3). Vollhardt utilized an elegant triple stereochemical labeling experiment to prove that the low-temperature photochemical equilibration of **4-ZZ** and **4-EE** occurs with a switch of the metal from one π -face of the diene to the other.¹³ The higher energies required for the related thermal process in **4** and **5** create some ambiguity in the detailed path of the thermal isomerization; although it is appealing to favor the prevailing envelope-flip mechanism, the possibility of structure **7** has not been excluded.

In the present study, we apply ab initio computational methods to elucidate the thermal envelope-flip manifold as a two-step inversion process and provide the first experimentally determined barrier to pairwise syn/anti interconversion in a group VIII metal–diene complex.

Computational Methods

Initial molecular structures have been optimized at the restricted Hartree–Fock (RHF) self-consistent field (SCF) level of theory with the aid of the analytically determined gradients and the search algorithms contained with GAMESS.¹⁸ Effects of dynamic correlation have been incorporated using hybrid density functional methodology (HDFT) using GAUSSIAN98.¹⁹ The HDFT methods employed Becke's three-parameter hybrid exchange functional²⁰ in combination with the nonlocal correlation provided by the Perdew (1991) expression, B3PW91.²¹ In the present study, relativistic effective core potentials (RECP)²² proposed by Hay and Wadt were used for the transition metal. The specific effective core potential/basis set combination used is commonly referred to by the acronym LANL2DZ, for Los Alamos National Laboratory 2-double- ζ . (The "2" indicating that the valence and "valence-1" shells are treated explicitly.) The LANL2DZ basis set is of double- ζ quality in the valence and "valence-1" shells,²³ while the RECP contains Darwin and mass–velocity contributions.^{22,24,25} This RECP has been determined to be a computationally very efficient and reliable approach to handling even third-row transition metal compounds.²⁶ In addition, for more accurate structures and energetics, calculations were carried out using a larger basis set we denote as LANL2DZ-1, which consists of the LANL2DZ basis set augmented with single f functions (exponents determined by Frenking and co-workers)^{27,28} on cobalt, and Dunning's cc-pVDZ (correlation consistent polarized valence double- ζ) basis set,²⁹ which is of [4s3p1d/3s2p1d/2s1p] quality, on H and the first- and second-row elements. Full geometry optimizations and subsequent second derivatives analyses were performed. Molecular orbital contour plots, used as an aid in the discussion of the results, were generated using the program 3D-PLTORB (San Diego, 3D version: 1997), and depicted using QMView.³⁰

Fragment Orbital Analysis

The limiting structures, **1** and **2** each represent 18-electron saturated valence shell complexes for cobalt. Simple fragment

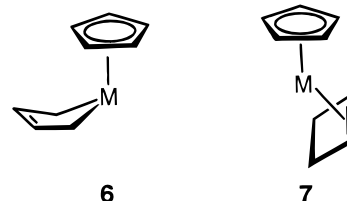


Figure 3. Two possible 16-electron intermediate in the syn,anti-isomerization process.

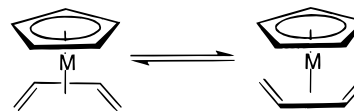


Figure 4. Conformers, I and I', due to metal cyclopentadienyl rotation.

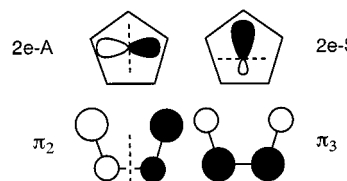


Figure 5. Frontier orbital matching to support a conformational preference in **1/2**.

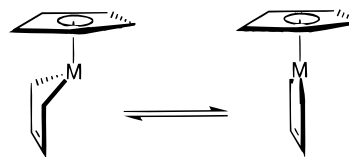


Figure 6. Pyramidal vs planar metallacyclopentene structure at cobalt.

frontier orbital analysis indicates that the half-filled degenerate 2e orbitals on the cyclopentadienylcobalt fragment interact with the π_2 and π_3 orbitals of the diene.³¹ The conformation of the cyclopentadienyl ring with respect to the diene fragment can be rationalized by the specific frontier interactions. One of the 2e orbitals, 2e-A, has its nodal plane coincident with the mirror plane of the molecule and is antisymmetric with regard to that symmetry element; by symmetry, the two sides of the orbital are equivalent in size and shape. The other 2e orbital, 2e-S, is orthogonal to the first, has its nodal plane perpendicular to the symmetry element, and is therefore symmetric with respect to the mirror; however, the lobes of the orbital are not symmetry related and therefore differ, albeit slightly, in size and shape. Of the diene orbitals, π_2 is antisymmetric and π_3 is symmetric with respect to the mirror; in both, the contribution from the terminal atomic orbitals is different from the internal atomic orbitals. Matching occurs between the filled 2e-S and the empty π_2 orbitals and between the empty 2e-A and the filled π_3 orbitals, the former pair having two slightly different combinations (I and I', cf. Figure 4) from which the one where the large lobes overlap dominates. The slight difference in overlap presages a minor conformational preference and low barrier to rotation (Figure 5).^{32,33}

Fragment orbital analysis of the coordinatively unsaturated 16-electron structure **6** leads to the qualitative prediction that the geometry about the metal will be pyramidal (Figures 6 and 7).^{34–36} This lowering of symmetry is rationalized by a similar analysis to that which predicted a slight conformational preference in **1/2**. The frontier orbitals from the organic ligand are the symmetric and antisymmetric combinations of the p orbitals on the terminal carbons. The metal still uses the 2e orbitals. One of the 2e orbitals can overlap with the antisymmetric

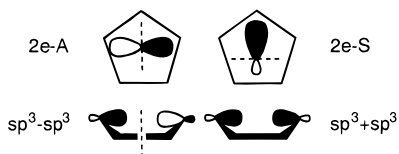


Figure 7. Frontier orbital matching to support pyramidity at cobalt.

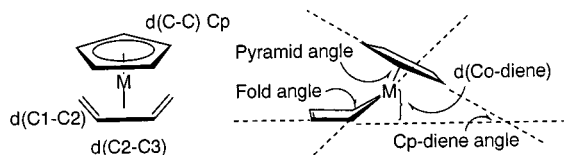


Figure 8. Various structural parameters for assessing the character of a diene complex.

combination from the ligand in either the idealized C_{2v} or C_s conformations; however, the other 2e orbital has a nodal plane that is incompatible with its combining with the symmetric combination from the organic ligand in the C_{2v} conformation. Distortion out of plane to a C_s geometry obviates that nodal problem and stabilizes the complex.

From this simple-minded analysis one realizes that two different stereochemical processes are necessary to interconvert the exo and endo hydrogens. One must not only flip over the five-member ring, but also invert the pyramid at the metal. In principle, these processes may occur in tandem or as part of a concerted double inversion. It is in regard to this issue that the ab initio computations are most helpful.

Structural Data in Support of the Envelope-Flip Mechanism

The interaction between the diene and the metal induces a rehybridization of the terminal carbon atoms as more of structure **1** character is mixed in. Structural and spectroscopic markers reveal the extent of this mixing. Following a standard Dewar–Chatt model for structure **2**,³⁷ one would expect elongation of the C=C double bonds, but little perturbation of the intervening C–C single bond; therefore, $d(C1-C2)$ would end up roughly equal to $d(C2-C3)$. On the other hand, structure **1** represents a complex with full-fledged carbon-to-metal σ bonds and a double bond between C2 and C3. In this extreme, $d(C1-C2)$ would be much long than $d(C2-C3)$. Conversely, observation of a structure with $d(C1-C2) \gg d(C2-C3)$ would support a strong contribution from structure **1**. Indeed, early-metal–diene complexes (Cp_2Hf and Cp_2Zr) show this latter bonding motif.^{6,12,38}

In addition to the bond lengths in the diene ligand, the angle between the base and the flap of the envelope (plane C1–C2–C3–C4 vs plane C1–M–C4) provides a useful parameter for how much type **1** character is present. For acute values of the dihedral angle, the complex is strongly dominated by type **2** whereas for obtuse dihedral angles there is a major contribution for type **1**. A combination of these geometrical parameters form a predictive correlation with the energy of syn/anti interconversion (Figure 8).^{9,12}

The direct $^{13}C-^{13}C$ one-bond couplings are also a good indication of bond distances in solution. In simple $Cp(\text{diene})$ –metal complexes, a coupling constant for the relationship in the terminal and internal diene bonds, and the internal Cp bonds, can be measured.³⁹ For complexes of structure **2**, one would expect the magnitude of all three coupling constants, J_{terminal} , J_{internal} , and J_{Cp} , to be similar; whereas significant contribution of structure **1** should cause the terminal and internal diene couplings to diverge with $J_{\text{terminal}} \ll J_{\text{internal}}$, J_{Cp} would remain

unchanged. Indeed, for group VIII metals the diene complexes show roughly equivalent couplings supporting a solution structure like **2**, and the coupling constants found in the early-metal–diene complexes are consistent with their adopting structures leaning toward structure **1**.³⁹ Given that these early-metal complexes lean toward structure **1** and display low barriers to syn,anti interconversion, it seems reasonable to conclude that the interconversion pathway is actually an envelope-flip mechanism. Indeed, Bürgi has shown that for early-metal– $Cp_2M(\text{diene})$ complexes a structure correlation can be developed that fits the dynamic behavior of these compounds to the degree of structural distortion.⁹

Elucidating the Path

Ab initio computations on $CpCo(\text{butadiene})$, predict a C_s symmetric η^4 -diene ground state conformation (**I**) consistent with structural type **2** (Table 1). The bond lengths are all similar (C1–C2 and C3–C4 = C2–C3). The terminal carbon atoms are only slightly pyramidalized and the envelope dihedral angle is distinctly acute (84.7°). Rotation of the Cp ring by 180° yields an alternative conformation (**I'**) that lies only 0.1 kcal/mol higher in energy, thus providing quantitative support for the small conformational preference predicted above. Computation of the C_s structure in which the metallacyclopentene is flat, and the Cp ring is rotated to match the mirror symmetry, yields a potential transition-state structure (α) 42.3 kcal/mol higher in energy than **I**. This value is in reasonable agreement with the estimate of the thermal barrier in **4-ZZ** (>39.5 kcal/mol); however, careful normal-mode analysis identified α as a saddle point with two imaginary frequencies. Following these imaginary modes led to two lower energy pairs of structures, (**A/A'**) and (**B/B'**); each of these structures proved to have one imaginary frequency and is a confirmed transition state. Whereas **A** and **A'** differ by 180° rotation of the Cp ring, **B** and **B'** are enantiomeric twist forms. From these transition states, one heads back to **I/I'** or to a new local minimum (**II/II'**), situated energetically 35.2 kcal/mol above the global minimum. These new minima represent the two conformational isomers of structural type **6**, differing only in the metal Cp torsion angle. In **II/II'** the C2–C3 bond is distinctly shorter than C1–C2 (C3–C4), the envelope dihedral is obviously obtuse (164.2°), and the end carbons display sp^3 angles. Notably, the ring is envelope puckered and the geometry at cobalt is pyramidal. Note that one major difference between **I** and **II** is the direction of pyramidity at the metal. One could reformulate the structure of **I** as an oddly distorted Co(III) metallacyclopentene, as depicted in limiting structure **1**; then the “free” site of the cobalt would be pointing directly at the back-bond (C2–C3) and can coordinate; however, in **II** the “free” site of the cobalt is pointing into space and is left unsaturated.

One can envision a couple of dynamic processes for intermediate **II** that could invert the configuration at cobalt. Given the character of **II** as an “envelope” five-membered ring, a pseudorotational manifold is feasible within which transition state **B** would be the key point through which the metal might invert. Alternatively, viewing **II** strictly as a distorted diene–metal complex evokes the possibility of pyramidal inversion through a simple sliding of the metal along the face of the diene. In the former the metal moves from one π -face to the other through the dynamic process (i.e. syn/anti exchange). In the later process, the metal remains solely on one face.

Considering all of the states enumerated and their possible interconnections, one arrives at a complete graph of dynamic processes which include ring flip, Cp ring rotation, pseudoro-

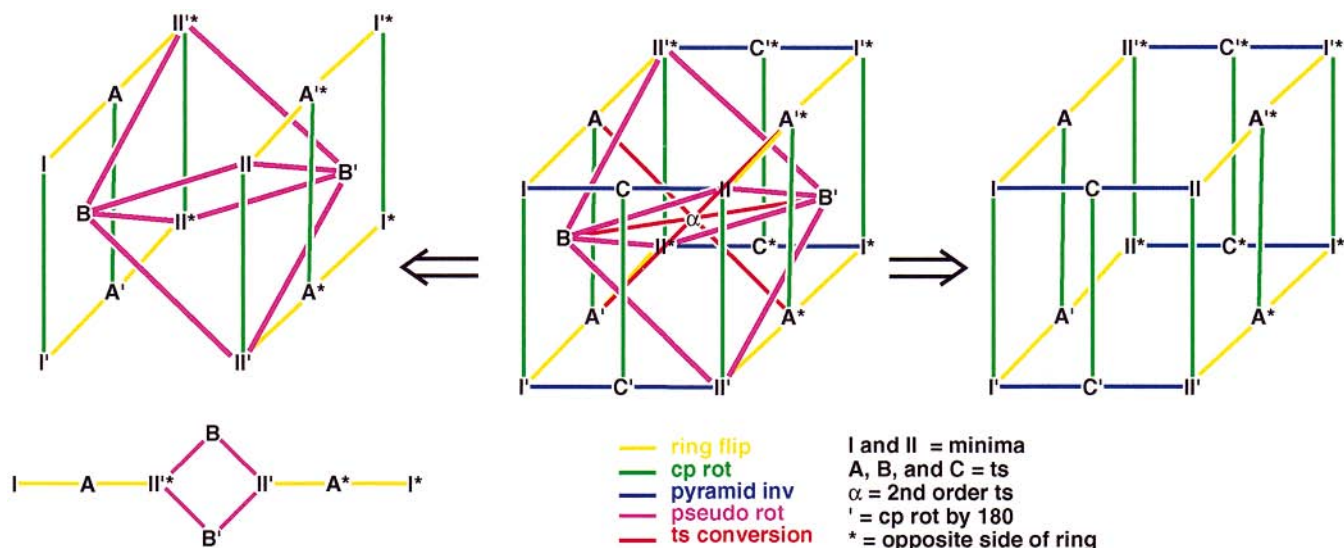


Figure 9. Graph theoretical consideration of the dynamic process: (center) the complete graph of considered states; (left) ring flip/pseudorotational inversion subgraphs; (right) ring flip/pyramidal inversion subgraph.

TABLE 1. Structures of the Principal Stationary Points on the “Envelope-Flip” Energy Hypersurface

structure	$d(\text{C1}-\text{C2})$	$d(\text{C2}-\text{C3})$	$d(\text{C}-\text{C})$ Cp_{avg} (Å)	$d(\text{Co}-\text{diene})$	fold angle (deg)	pyramid angle (deg)	Cp-diene angle (deg)
I	1.427	1.422	1.429	1.508	83.5	20.4	13.9
I'	1.422	1.426	1.429	1.509	83.5	20.6	165.9
II	1.490	1.345	1.428	0.375	164.7	31.0	43.7
II'	1.485	1.349	1.428	0.416	163.0	30.9	137.9
A	1.503	1.341	1.427	0.692	150.6	34.6	95.15
A'	1.503	1.340	1.426	0.629	153.5	33.7	82.8
B/B''	1.428	1.384	1.428	0.071	176.8	6.5	85.9
C	1.478	1.353	1.415	0.438	162.2	26.9	45.4
α	1.513	1.348	1.440	0.000	180.0	0.0	90.0

TABLE 2. Energies (hartrees) (and relative kcal/mol) of the Principal Stationary Points on the “Envelope-Flip” Energy Hypersurface

structure	B3LYP/LANL2DZ	B3LYP/LANL2DZ+1	character	imag freq
I	-494.553 572 (0.0)	-494.640 156 (0.0)	0	
I'	-494.553 488 (0.05)	-494.639 912 (0.15)	0	
II	-494.503 499 (31.4)	-494.584 043 (35.2)	0	
II'		-494.583 975 (35.2)	0	
A	-494.500 250 (33.4)	-494.578 890 (38.4)	1	-140
A'		-494.576 948 (39.6)	1	-136
B/B''		-494.578 487 (38.6)	1	-116
C		-494.582 984 (35.9)	1	-22
α	-494.491 460 (38.9)	-494.572 728 (42.3)	2	-216, -93

tational inversion, pyramidal inversion, and transition through a second-order transition state (Figure 9). From that complete graph a subgraph for either the ring flip/pseudorotational inversion process (Figure 10) or the ring flip/pyramidal inversion process (Figure 11) can be extracted. Evaluating the energetics along the graphical paths elucidates the energy barrier.

With all of these structures in hand, one can construct reaction energy graphs in which one coordinate is ring-flipping and the other is inversion at cobalt (Figures 10 and 11). In one case, the ring flip drops one into a pseudorotational manifold through which inversion at cobalt is effected and then another ring flip completes the isomerization. Alternatively, from global minimum I the molecule can traverse either TS A to minimum II' by flipping the ring or TS C to minimum II by inverting at cobalt. The latter looks formally like a slipping of the diene parallel to the Cp ring, whereas the former looks like the ring is standing up normal to the Cp ring and turning over. Precise interpretation of the energy surface requires some additional liberation of the Cp ring, but this detail does not add any significant mechanistic insight or provide a major energetic

perturbation (<0.01 kcal/mol). What is striking is that after the initial formation of II the energy hypersurface is flat and the dynamics are extremely fluxional with access to a number of closely lying conformational states. In addition, no matter the specifics of the two mechanisms articulated above, the α state, representing a concerted ring-flip and cobalt inversion is avoided in favor of a multistep ring-flip/cobalt inversion process. The rate-determining transition state rests 38–39 kcal/mol above the global minimum, within reasonable agreement with the experimental estimate (>39.5 kcal/mol).¹³

The present analysis also allows us to address the photochemically accelerated syn/anti isomerization reported by Vollhardt.¹³ Group VIII metals in saturated complexes with ligands capable of undergoing cyclopentadienyl “ring-slippage”⁴⁰ are notorious for avoiding dissociative mechanisms. Indeed, substitution in such systems was assumed to proceed exclusively by associative pathways.^{41,42} Bergman provided an important counterexample to this expectation by inducing a dissociative substitution to occur photochemically.³⁵ Oddly enough, one can view the syn/anti isomerization in the CpCo(diene) complex as

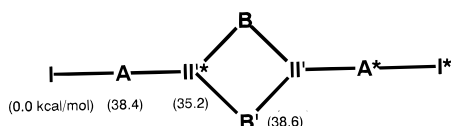


Figure 10. Scheme and energetics for the ring-flip/pseudorotational inversion pathway.

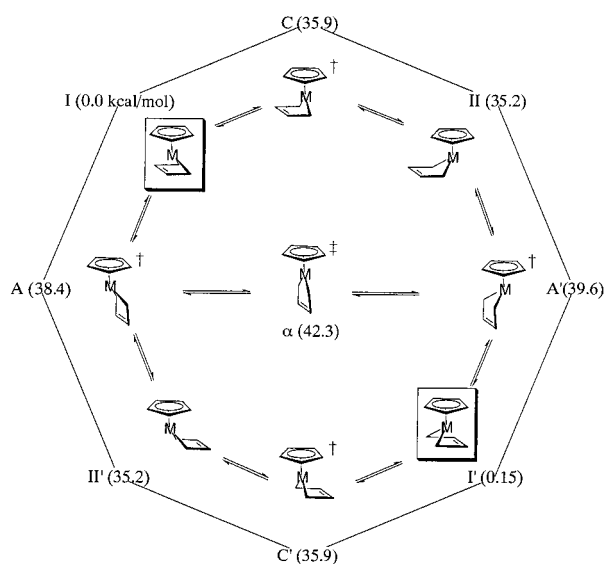


Figure 11. Scheme and energetics for the two-step ring flip/pyramidal inversion syn/anti isomerization that interconverts **I** with **I'**.

an internal dissociative substitution process. From that perspective, **II**¹⁵ would be the “dissociated state.” Assuming that Vollhardt’s photochemistry sets up a photostationary equilibrium between **I** and **II**, then syn/anti isomerization could occur with a thermal barrier of less than 5 kcal/mol. Even with a tiny equilibrium toward **II**, this barrier would account for the isomerization rates seen at $-96\text{ }^{\circ}\text{C}$.

CpCobalt(η^2 -cyclobutene)

Although the details of the metal-induced electrocyclic ring closure to CpCo(η^2 -cyclobutene) is beyond the present study, it was informative to look at the structure and energy of the type **7** complex. Structure **7** was found to be comparably high in energy, comparable with the transition states **A**(**A'**) and **B**(**B'**), but lower in energy than α . Cobalt is again pyramidal in **7** and favors a structure that minimizes the steric interactions between the Cp and the cyclobutene rings. Unfortunately, the energetics are not so distinctive that one can exclude an isomerization path involving **7**; however, with the data at present in hand, one would disfavor such a path. Investigation of the details of the electrocyclic mechanism are continuing, along with an attempt to understand how substituent effects might perturb the apparent subtle balance of energies favoring the envelope-flip over the electrocyclic mechanism.

Experimental Observation of Isomerization between **5d-EZ** and **5d-ZE**

Access to the cobalt diene complexes (**5**) allows for the first quantitative assessment of the activation energy for a pairwise syn/anti interconversion in a group VIII complex. The three diene isomers **5d-ZZ**, **5d-ZE**, and **5d-EZ** (Scheme 2) have been prepared from reaction of the cobalt–alkyne complex (η^5 - C_5H_5)(PPh_3)Co(η^2 -TMSC \equiv CSO $_2$ Ph) and butenyl diazoacetate in benzene solution at room temperature. The three isomers were

readily separated by chromatography and have been characterized by NMR spectroscopy, HRMS, and combustion analysis. The ZZ isomer of **5d** proved to be stable in benzene- d_6 solution even at $130\text{ }^{\circ}\text{C}$ over the course of 14 days; however, heating a benzene solution of **5d-ZE** at $110\text{ }^{\circ}\text{C}$ in the dark led to slow formation of **5d-EZ** in 97% isolated yield. There was no spectroscopic evidence (<3%) for formation of either the EE or ZZ isomers of **5d**. When acetone- d_6 solutions of **5d-ZE** were exposed to sunlight at room temperature, a 22:1 ratio of EZ:ZE isomers was generated within 12 h. The isomerization of **5d-ZE** to **5d-EZ** can be conveniently followed by ^1H NMR spectroscopy in benzene- d_6 from integration of the H-anti resonances at δ 1.49 (**5d-ZE**) and 1.57 (**5d-EZ**). Using the rates found at four temperatures between 90 and $119\text{ }^{\circ}\text{C}$ allowed us to determine that $E_{\text{act}} = 31\text{ kcal mol}^{-1}$, a value more than 9 kcal mol^{-1} lower than that determined through experiment¹³ and computation for the parent diene complex, **4**. It is clear from this result that diene substituents exert a significant effect on the barrier to syn/anti interconversion processes.⁴³ The nature of this effect awaits additional experimental and computational studies.

Experimental Section

General. IR spectra were recorded on a Mattson-Galaxy 2020 FT-IR or a Nicolet Magna-IR 550 spectrometer. Melting points were determined on an Electrothermal melting point apparatus and are reported uncorrected. NMR spectra were recorded on a GE QE 300 (^1H 300 MHz, ^{13}C 75.5 MHz) spectrometer. Chemical shifts were referenced to residual protio-solvent signal. FAB mass spectra were performed at the University of California, Riverside Mass Spectroscopy Facility. Elemental analyses were performed by Desert Analytics or Galbraith Laboratories, Inc. Chromatography was performed in the air. Benzene, hexanes, and diethyl ether were distilled from sodium/benzophenone ketyl under an atmosphere of nitrogen. The cobalt–alkyne complex (η^5 - C_5H_5)(PPh_3)Co(η^2 -TMSC \equiv CSO $_2$ -Ph)⁴⁴ and butenyl diazoacetate⁴⁵ were prepared by literature procedures.

Preparation of (η^5 - C_5H_5)Co[η^4 -CH(CO $_2$ R)=C(SO $_2$ Ph)-C(TMS)=CH(CO $_2$ R)] (5d**, R = C_4H_7).** A benzene solution (30 mL) of the cobalt–alkyne complex (η^5 - C_5H_5)(PPh_3)Co(η^2 -TMSC \equiv CSO $_2$ Ph) (312 mg, 0.5 mmol) and $\text{N}_2\text{CHCO}_2\text{C}_4\text{H}_7$ (350 mg, 2.5 mmol) was stirred under a nitrogen atmosphere at room temperature for 24 h. Chromatography (silica gel, 20% ethyl acetate/hexanes) led to the collection of four red bands. The first band yielded 129 mg of a red oil, which was recrystallized from hexanes ($0\text{ }^{\circ}\text{C}$) to give **5d-ZZ** (90 mg, 30%) as a crystalline solid. The second band gave **5d-EZ** (28 mg, 10%) as a red oil. The third band gave 105 mg of a red oil which was recrystallized from hexanes ($0\text{ }^{\circ}\text{C}$) to give **5d-ZE** (70 mg, 24%) as a crystalline solid. The fourth band was identified as a cobaltacyclobutene complex.

For **5d-ZZ**: mp 136.5 – $137\text{ }^{\circ}\text{C}$; ^1H NMR (C_6D_6 , 300 MHz) δ 0.40 (s, 9 H, Si(CH_3) $_3$), 0.01 (s, 1 H, H_{anti}), 0.85 (s, 1 H, H_{anti}), 1.92 (m, 2 H, OCH $_2$ CH $_2$), 2.25 (m, $J = 6.6\text{ Hz}$, 2 H, OCH $_2$ CH $_2$), 3.94 (m, 2 H, OCH $_2$), 4.02 (t, $J = 6.6\text{ Hz}$, 2 H, OCH $_2$), 4.95 (m, 4 H, CH=CH $_2$), 5.32 (s, 5 H, C_5H_5), 5.46 (m, 1 H, CH=CH $_2$), 5.69 (m, 1 H, CH=CH $_2$), 6.96 (m, 3 H, C_6H_5), 8.00 (m, 2 H, C_6H_5); $^{13}\text{C}\{^1\text{H}\}$ NMR (C_6D_6 , 75.5 MHz) δ 32.80 and 33.64 (OCH $_2$ CH $_2$), 49.45 and 57.02 (C=CHCO $_2$), 63.54 and 64.60 (OCH $_2$), 86.74 (C_5H_5), 88.49 and 96.66 (C=CHCO $_2$), 116.78 and 117.28 (CH=CH $_2$), 125.97 (C_m), 128.54 (C_o), 132.07 (C_p), 134.61 and 134.84 (CH=CH $_2$), 143.90 (C_i), 170.10 and 174.49 (CO $_2$); HRMS(FAB) m/z calcd for $\text{C}_{28}\text{H}_{35}\text{O}_6\text{CoSSi}$:

586.1255, obsd: 586.1254; Anal. Calcd for $C_{28}H_{35}O_6CoSSi$: C, 57.33; H, 6.01. Found: C, 57.60; H, 5.88.

For **5d-EZ**: 1H NMR (C_6D_6 , 300 MHz) δ 0.45 (s, 9 H, Si(CH₃)₃), 1.57 (s, 1 H, H_{anti}), 2.16 (m, 4 H, CH₂CH=CH₂), 3.50 (m, 1 H, OCH₂), 3.98 (t, $J = 6.6$ Hz, 2 H, OCH₂), 4.10 (m, 1 H, OCH₂), 4.88 (s, 1 H, H_{syn}), 4.95 (m, 4 H, CH=CH₂), 5.07 (s, 5 H, C₅H₅), 5.63 (m, 2 H, CH=CH₂), 6.90 (m, 3 H, C₆H₅), 7.99 (m, 2 H, C₆H₅); $^{13}C\{^1H\}$ NMR (C_6D_6 , 75.5 MHz) δ 3.33 (Si(CH₃)₃), 33.58 (br, probably two resonances, OCH₂CH₂), 42.38 and 46.58 (C=CHCO₂), 63.54 and 63.63 (OCH₂), 85.90 (C₅H₅), 98.66 and 101.16 (C=CHCO₂), 117.09 and 117.19 (CH=CH₂), 125.60 (C_m), 128.98 (C_o), 132.16 (C_p), 134.42 and 134.70 (CH=CH₂), 144.22 (C_i), 171.25 and 175.73 (CO₂); HRMS(FAB) m/z calcd for $C_{28}H_{35}O_6CoSSi$: 586.1255, obsd: 586.1228; Anal. Calcd for $C_{28}H_{35}O_6CoSSi$: C, 57.33; H, 6.01. Found: C, 57.48; H, 5.95.

For **5d-ZE**: IR (thin film) 1717, 1697 cm^{-1} ; 1H NMR (C_6D_6 , 300 MHz) δ 0.55 (s, 9 H, Si(CH₃)₃), 1.49 (s, 1 H, H_{anti}), 1.83 (q, $J = 6.3$ Hz, 2 H, CH₂CH=CH₂), 2.11 (q, $J = 6.3$ Hz, 2 H, CH₂CH=CH₂), 3.44 (dt, $J = 10.5, 6.6$ Hz, 1 H, OCH₂), 3.61 (dt, $J = 10.5, 6.3$ Hz, 1 H, OCH₂), 3.75 (dt, $J = 10.8, 6.3$ Hz, 1 H, OCH₂), 3.79 (s, 1 H, H_{syn}), 3.99 (dt, $J = 10.8, 6.3$ Hz, 1 H, OCH₂), 4.92 (m, 4 H, CH=CH₂), 4.94 (s, 5 H, C₅H₅), 5.43 (m, 1 H, CH=CH₂), 5.62 (m, 1 H, CH=CH₂), 6.84 (m, 3 H, C₆H₅), 7.94 (m, 2 H, C₆H₅); $^{13}C\{^1H\}$ NMR (C_6D_6 , 75.5 MHz) δ 2.13 (Si(CH₃)₃), 33.22 and 33.69 (OCH₂), 40.11 and 44.83 (C=CHCO₂), 63.21 and 63.31 (OCH₂), 85.02 (C₅H₅), 89.88 and 114.00 (C=CHCO₂), 116.93 and 117.00 (CH=CH₂), 128.00 (C_m), 128.47 (C_o), 132.16 (C_p), 134.42 and 134.83 (CH=CH₂), 142.69 (C_i), 172.04 and 172.27 (CO₂); HRMS(FAB) m/z calcd for $C_{28}H_{35}O_6CoSSi$: 586.1255, obsd: 586.1262; Anal. Calcd for $C_{28}H_{35}O_6CoSSi$: C, 57.33; H, 6.01. Found: C, 57.60; H, 5.75.

Acknowledgment. This work is supported by the US National Science Foundation (CHE-9628565; CHE-9520213; ASC-9212619), the National Biomedical Computational Resource, the Grand Challenge Program (computer time), and the Petroleum Research Fund of the American Chemical Society. The authors also acknowledge Kent Wilson, the honoree of this issue, for being an inspirational colleague and one of the world's most creative scholars; we gladly dedicate this paper to him.

References and Notes

- van't Hoff, J. H. *La Chimie dans l'Espace*; P. M. Bazendijk: Rotterdam, 1875.
- Glasstone, S.; Laidler, K. L.; Eyring, H. *Theory of Rate Processes*; McGraw-Hill: New York, 1941.
- Kistiakowsky, G. B.; Smith, W. R. *J. Am. Chem. Soc.* **1938**, *58*, 766.
- Anderson, W. F.; Bell, J. A.; Diamond, J. M.; Wilson, K. R. *J. Am. Chem. Soc.* **1958**, *80*, 2384–6.
- Wakatsuki, Y.; Aoki, K.; Yamazaki, H. *J. Chem. Soc., Dalton Trans.* **1982**, 89–94.
- Smith, G. M.; Suzuki, H.; Sonnenberg, D. C.; Day, V. W.; Marks, T. J. *Organometallics* **1986**, *5*, 549–61, and references therein.
- Yasuda, H.; Tatsumi, K.; Nakamura, A. *Acc. Chem. Res.* **1985**, *18*, 120–6.
- Krüger, C.; Müller, G.; Erker, G.; Dorf, U.; Engel, K. *Organometallics* **1985**, *4*, 215–23.
- Bürgi, H. B.; Dubler-Stuedle, K. C. *J. Am. Chem. Soc.* **1988**, *110*, 4953–4957.
- O'Connor, J. M.; Chen, M.-C.; Frohn, M.; Rheingold, A. L.; Guzei, I. A. *Organometallics* **1997**, *16*, 5589–91.
- O'Connor, J. M.; Chen, M.-C.; Rheingold, A. L. *Tetrahedron Lett.* **1997**, *38*, 5241–4.
- King, J. A., Jr. Ph.D. Thesis, UC Berkeley, Berkeley, CA, 1983.
- Eaton, B.; King, J. A., Jr.; Vollhardt, K. P. C. *J. Am. Chem. Soc.* **1986**, *108*, 1359–60.
- Eaton, B. Ph.D. Thesis, UC Berkeley, Berkeley, CA, 1986.
- Faller has suggested an intermediate related to **6** for a syn/anti isomerization process in a molybdenum diene complex, see: Faller, J. W.; Rosan, A. M. *J. Am. Chem. Soc.* **1977**, *99*, 4858–9.
- Pinhas, A. R.; Carpenter, B. K. *J. Chem. Soc., Chem. Commun.* **1980**, 15–17.
- Slegeir, W.; Case, R.; MvKennis, J. S.; Pettit, R. *J. Am. Chem. Soc.* **1974**, *96*, 287–8.
- Schmidt, M. W.; Baldrige, K. K.; Boatz, J. A.; Elbert, S. T.; Gordon, M. S.; Jensen, J. H.; Koseki, S.; Matsunaga, N.; Nguyen, K. A.; Su, S.; Windus, T. L.; Elbert, S. T. *J. Comput. Chem.* **1993**, *14*, 1347.
- Frisch, M. J.; Trucks, G. W.; Schlegel, H. B.; Gill, P. M. W.; Johnson, B. G.; Robb, M. A.; Cheeseman, J. R.; Keith, T. A.; Petersson, G. A.; Montgomery, J. A.; Raghavachari, K.; Al-Laham, M. A.; Zakrzewski, V. G.; Ortiz, J. V.; Foresman, J. B.; Cioslowski, J.; Stefanov, B. B.; Nanayakkara, A.; Challacombe, M.; Peng, C. Y.; Ayala, P. Y.; Chen, W.; Wong, M. W.; Andres, J. L.; Replogle, E. S.; Gomperts, R.; Martin, R. L.; Fox, D. J.; Binkley, J. S.; DeFrees, D. J.; Baker, J.; Stewart, J. P.; Head-Gordon, M.; Gonzalez, C.; Pople, J. A. *GAUSSIAN94-DFT*, Revision B.1 Gaussian, Inc.: Pittsburgh, PA, 1994.
- Becke, A. D. *J. Chem. Phys.* **1993**, *98*, 5648–5652.
- Perdew, J. P.; Wang, Y. *Phys. Rev. B* **1992**, *45*, 13244.
- Hay, P. J.; Wadt, W. R. *J. Chem. Phys.* **1985**, *82*, 270–283.
- Dunning, T. H., Jr.; Hay, P. J. *Modern Theoretical Chemistry*; Plenum: New York, 1976.
- Wadt, W. R.; Hay, P. J. *J. Chem. Phys.* **1985**, *82*, 284–298.
- Hay, P. J.; Wadt, W. R. *J. Chem. Phys.* **1985**, *82*, 299–310.
- Seigbahn, P. E. M. *Adv. Chem. Phys.* **1996**, *93*, 333.
- Ehlers, A. W.; Böhme, M.; Dapprich, S.; Gobbi, A.; Höllwarth, A.; Jonas, V.; Köhler, K. F.; Stegmann, R.; Veldkamp, A.; Frenking, G. *Chem. Phys. Lett.* **1993**, *208*, 111.
- Höllwarth, A.; Böhme, M.; Dapprich, S.; Ehlers, A. W.; Gobbi, A.; Jonas, V.; Köhler, K. F.; Stegmann, R.; Veldkamp, A.; Frenking, G. *Chem. Phys. Lett.* **1993**, *208*, 237.
- Dunning, T. H. *J. Chem. Phys.* **1989**, *90*, 1007.
- Baldrige, K. K.; Greenberg, J. P. *J. Mol. Graphics* **1995**, *13*, 63–66.
- Albright, T. A.; Geiger, W. E., Jr.; Moraczewski, J.; Tulyathan, B. *J. Am. Chem. Soc.* **1981**, *103*, 4787–94.
- Albright, T. A.; Hofmann, P.; Hoffmann, R. *J. Am. Chem. Soc.* **1977**, *99*, 7546.
- Baldrige, K. K.; Siegel, J. S. *J. Phys. Chem.* **1996**, *100*, 6111–6115.
- Hofmann, P.; Padmanabhan, M. *Organometallics* **1983**, *2*, 1273–84.
- Janowicz, A. H.; Bryndza, H. E.; Bergman, R. G. *J. Am. Chem. Soc.* **1981**, *103*, 1516–8.
- Costuas, K.; Saillard, J.-Y. *Organometallics* **1999**, *18*, 2505–2512.
- Lukehart, C. *Fundamental Transition Metal Organometallic Chemistry*; Brooks/Cole Publishing: Monterey, CA, 1985.
- Benn, R.; Schroth, G. *J. Organomet. Chem.* **1982**, *228*, 71–85.
- Benn, R.; Rufinska, A. *J. Organomet. Chem.* **1987**, *1987*, 305–12.
- O'Connor, J. M.; Casey, C. P. *Chem. Rev.* **1987**, *87*, 307–18.
- Schuster-Woldan, H.-G.; Basolo, F. *J. Am. Chem. Soc.* **1966**, *99*, 1657.
- Basolo, F. *Coord. Chem. Rev.* **1982**, *43*, 7.
- For related work on early-metal diene complexes, see: Erker, G.; Engel, K.; Krüger, C.; Müller, G. *Organometallics* **1984**, *3*, 128–33.
- O'Connor, J. M.; Ji, H.; Iranpour, M.; Rheingold, A. L. *J. Am. Chem. Soc.* **1993**, *115*, 1586–88.
- Doyle, M. P.; Austin, R. E.; Bailey, A. S.; Dwyer, M. P.; Dyatkin, A. B.; Kalinin, A. V.; Kwan, M. M. Y.; Liras, S.; Oalman, C. J.; Pieters, R. J.; Protopopova, M. N.; Raab, C. E.; Roos, G. H. P.; Zhou, Q. L.; Martin, S. F. *J. Am. Chem. Soc.* **1995**, *117*, 5763.